Ground State and Excited State H-Atom Temperatures in a Microwave Plasma Diamond Deposition Reactor

A. Gicquel, M. Chenevier, Y. Breton, M. Petiau, J. Booth, K. Hassouni

Ground State and Excited State H-Atom Temperatures in a Microwave Plasma Diamond Deposition Reactor

A. Gicquel ([1,*]), M. Chenevier ([2]), Y. Breton ([1]), M. Petiau ([1]), J.P. Booth ([2]) and K. Hassouni ([1])

([1]) Laboratoire d'Ingéniérie des Matériaux et des Hautes Pressions (**), Université Paris-Nord, avenue J.B. Clément, 93430 Villetaneuse, France
([2]) Laboratoire de Spectrométrie Physique (***), Université Joseph Fourier de Grenoble, B.P. 87, 38402 Saint Martin d'Hères Cedex, France

(Received 22 February 1996, revised 14 June 1996, accepted 24 June 1996)

PACS.52.70.-m – Plasma diagnostic techniques and instrumentation
PACS.52.70.Kz – Optical (ultraviolet, visible, infrared) measurements

Abstract. — Ground electronic state and excited state H-atom temperatures are measured in a microwave plasma diamond deposition reactor as a function of a low percentage of methane introduced in the feed gas and the averaged input microwave power density. Ground state H-atom temperature (T_H) and temperature of the H-atom in the $n = 3$ excited state ($T_{H\alpha}$) are obtained from the measurements respectively of the excitation profile by Two-photon Allowed transition Laser Induced Fluorescence (TALIF) and the H_α line broadening by Optical Emission Spectroscopy (OES). They are compared to gas temperatures calculated with a 1D diffusive non equilibrium H_2 plasma flow model and to ground electronic state rotational temperatures of molecular hydrogen measured previously by Coherent Anti-Stokes Raman Spectroscopy.

1. Introduction

Spatially resolved spectroscopic analysis of the plasma provides measurements of local characteristics in the plasma and at the plasma/surface interface (temperatures, concentrations). Their knowledge allows validation of models leading to an increased understanding of the phenomena. The spectroscopic analysis also provides a mean for monitoring the reactors. However, since the control of industrial reactors by laser spectroscopy is unrealistic, the development of measurements by Optical Emission Spectroscopy (OES), associated to their calibration by laser diagnostics techniques, is needed.

Measurements of ground state H-atom temperature by Two-photon Allowed transition Laser Induced Fluorescence (TALIF) have been already reported in the literature [1–6]. As well, measurements of excited states H-atom temperature have been performed, in particular some of them, in plasma reactors used for diamond deposition [7–9]. However, to our knowledge, no comparison between these measurements performed under experimental conditions typical for

(*) Author for correspondence
(**) CNRS-UPR 1311
(***) CNRS-URM C5588

diamond deposition (pressure higher than 2 000 Pa) have been yet discussed. In addition, at pressure of around 100 Pa, Amorim *et al.* [1] and Rousseau *et al.* [4] have demonstrated that the H-atom temperature is much higher than the gas temperature owing to the production of hot H atoms from a dissociative excitation process involving collisions between H_2 molecules and electrons. In this paper, we report spectroscopic measurements performed in microwave plasmas operating under conditions typical for diamond deposition. A comparison between measurements of ground state and excited state H-atom temperatures, measured from Doppler broadening is presented. Ground state H-atom temperature (T_H) is measured by TALIF, and temperature of H-atom in the $n = 3$ excited state (T_{H_α}) by OES. Stark and pressure broadenings have been considered for the estimation of the $n = 3$ excited H-atom temperature from OES measurements. These have been also compared to gas temperatures calculated with a 1D diffusive non equilibrium H_2 plasma flow model [10,11], and to rotational temperatures of molecular hydrogen in its ground electronic state measured previously by Coherent Anti-Stokes Raman Spectroscopy (equal to the gas temperature) [12,13]. Their variations as a function of a low percentage of methane introduced in the feed gas (up to 5%) and as a function of the averaged microwave power density are presented.

2. Experimental Set-Up and Diagnostics

The microwave plasma diamond deposition reactor, made of a silica bell jar is working under moderated pressure. It has been already presented elsewhere [12]. The feed gas is a mixture of a few percentage of methane (0-5%) in hydrogen, as conventionally used for diamond deposition. The feed gas is activated by either a 1200 W or a 6 kW, 2.45 GHz SAIREM microwave generator. 5 cm diameter ⟨100⟩ single crystal silicon wafers covered by a polycrystalline untextured diamond film were placed inside the plasma ball, in such a way to keep constant the interacting system ($H_2 + CH_4$ plasma/diamond surface).

The averaged input microwave power density defined as the input microwave power over the volume of the plasma obtained in absence of substrate holder (plasma ball) (in W cm^{-3}) was changed by a simultaneous variation of the pressure and the microwave power. By changing only either the power or the pressure makes the plasma volume varying which is not desirable since diamond deposition has to be carried out on a constant surface of 5 centimeter in diameter. In addition, at a given pressure, an increase in the power can lead eventually to the formation of a second plasma at the top inside of the bell jar, which is also not desirable. By a simultaneous variation of both pressure and power, the plasma volume as well as the power over the total density (P_{MW}/n) (where P_{MW} is the injected power in W and n, the total density, in cm^{-3}) were kept as constant as possible, respectively at 65 cm^3 and between 6 to 7 $\times$ 10^{-15} W cm^3/molecules. The relative error made on the plasma volume has been estimated at around 2%, that on the power density at around 10%, owing to the uncertainty on the injected power (injected and reflected powers are measured only by the constructor power-meters). The absorbed power is not known, however, according to Grotjohn *et al.* [14], it should be close to the net injected power. Since the plasma volume is kept constant, at a given axial location in the plasma, the averaged line-of-sight intensities are measured always with the same plasma volume. The power was varied from 400 W to 2 400 W, and the pressure from 800 Pa to 14 000 Pa. The power density was varied from 4.5 W cm^{-3} to 37 W cm^{-3}

Depending on the plasma conditions, in particular the averaged microwave power density, heating or cooling of the substrate holder was used to maintain the substrate temperature constant at the chosen temperature (900 °C for this study), which was measured by a bichromatic pyrometer.

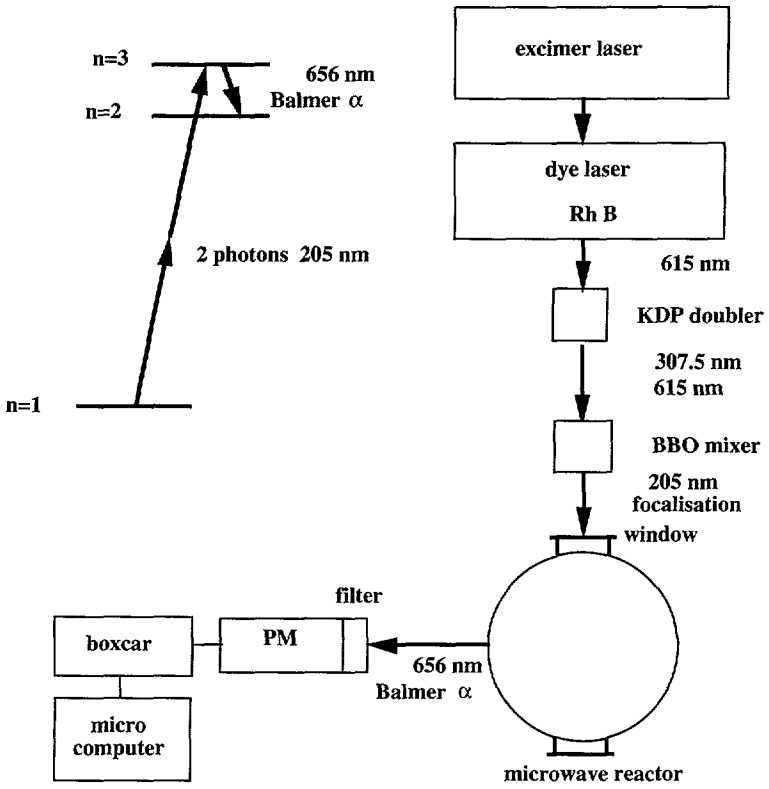

Fig. 1. — Two photons Allowed Transition Laser Induced Fluorescence (TALIF) experimental block.

2.1. Two Photon L.I.F. Technique (TALIF). — Two photons allowed transition laser induced fluorescence (TALIF) [5,6,13] measurements were conducted in the reactor equipped with two U.V. grade silica windows allowing transmission of 205 nm light. The whole reactor was accurately translated vertically and horizontally with respect to the laser beam in order to obtain axial and radial profiles. The spatial resolution is estimated at 0.5 mm.

The system used to generate the light at about 205 nm consists of a pulsed excimer laser (XeCl) emitting at 308 nm. This excimer pumps a dye laser composed of a tunable oscillator and of an amplifier. With rhodamine B an intense beam is obtained at 615 nm which is frequency doubled in a KDP crystal to give 307.5 nm. Mixing with the residual beam at 615 nm in a BBO crystal, produces the 205 nm beam, with a repetition rate of 10 Hz and a pulse duration of about 25 ns, the energy by pulse and the linewidth are typically of 50 μJ and 0.0025 nm respectively. The whole laser system is computer controlled and allows wavelength scanning over a few nm. In our experiment a scan of 0.030 nm is sufficient to cover the line profile with 90 steps. The profile line is obtained with a laser wavelength varying from 205.065 nm to 205.095 nm. The fluorescence light is collected at 90° to the laser beam by two lenses and detected directly by a photomultiplier in front of which an interference filter centered at 656.5 nm is used to eliminate scattered laser light. The resulting signal is proceeded by a boxcar integrator and sent to a personal computer. The fluorescence signal is averaged over 20 laser shots for each wavelength step, thus a scan takes about 3 minutes. A block diagram of the experimental set-up is presented in Figure 1. Under the experimental conditions, the

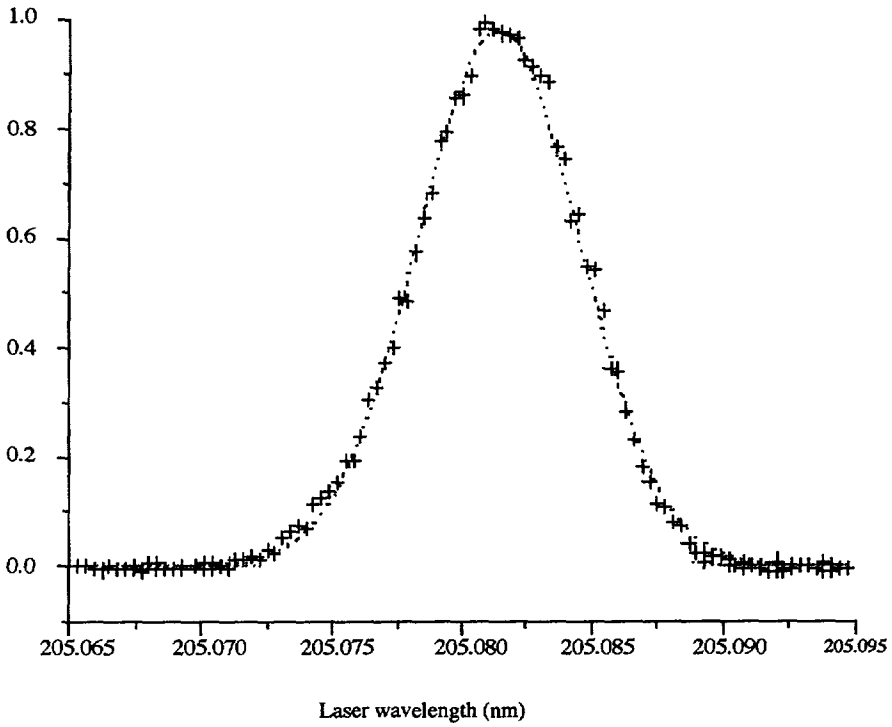

Fig. 2. — Example of a Doppler broadened TALIF Fluorescence signal.

observed two-photon line profile (Fig. 2) is Doppler broadening dominated. Its full-width at half-maximum is directly related to the translational temperature of the atoms, and its area to their concentration.

Width and Temperature. — As atomic hydrogen is the lightest atom, the Doppler broadening line is particularly large, and this is therefore advantageous for temperature measurements from line profiles. By measuring the Doppler linewidth $\Delta\lambda_D$ (full width at half maximum, FWHM) of the fluorescence excitation profile, the H-atom temperature can be determined using the formula:

$$\frac{\Delta\lambda_D}{\lambda_0} = \frac{2}{c}\sqrt{\frac{2kT\ln 2}{m}} = 7.16 \times 10^{-7}\sqrt{\frac{T}{M}} \tag{1}$$

where c is the speed of light, k the Boltzmann constant, m is the mass of the atom, T is the temperature of the atom and M is the mass of the atom in AMU.

We estimate the magnitude of $\Delta\lambda_D$ by applying equation (1) to the H atom at 1500 K for the doubled $1^2S \rightarrow 3^2S(^2D)$ H atom transition, *i.e.* for $\lambda_0 = 205.14$ nm in vacuum (205.082 in air). A value of 0.0057 nm is obtained for $\Delta\lambda_D$. For the experimental conditions used for TALIF measurements, *i.e.* pressure varying from 1400 to 5 200 Pa, the atomic fine structure and the collisional broadening, which are of the order of 0.00015 nm for the transition involved, have been neglected. Therefore, the line profile is considered as a pure Gaussian. By fitting

the experimental profile with a Gaussian profile,

$$f(\lambda) = a + b\exp\left[-4\ln 2\left(\frac{\lambda - \lambda_0}{\Delta\lambda_R}\right)^2\right] \tag{2}$$

we obtained four parameters $(a, b, \lambda_0, \Delta\lambda_R)$, where $\Delta\lambda_R$ is the resulting LIF signal FWHM. $\Delta\lambda_R$ is directly related to the Doppler broadening, $\Delta\lambda_D$, and to the laser width, $\Delta\lambda_L$, by the relation:

$$\Delta\lambda_{R^2} = \Delta\lambda_{D^2} + \Delta\lambda_{L^2} \tag{3}$$

We can then obtain $\Delta\lambda_D$ and estimate the H-atom temperature. For the determination of $\Delta\lambda_L$ (laser width) we performed measurements with a room temperature atomic hydrogen source and a value of 0.0025 nm was obtained.

Owing to experimental difficulties, the error in the measurements from the long-term reproducibility is quite large, it is estimated at ±250 K, at 2 000 K.

2.2. Optical Emission Spectroscopy (OES). — A Jobin Yvon THR 1000 mounted with a 1800 groves per mm grating, blazed at 450 nm and equipped with a photomultiplier (Hamamatsu R 3896) and a Pelletier effect cooling system allowed us (with spectrometer slits of 1 500 nm (1.5 μm)) to reach a resolution of around 5 pm (0.005 nm), making possible measurements of Doppler broadening on H atoms during the radiative decay from the $n = 3$ to $n = 2$ fluorescence line (H_α). The light emitted from the plasma was collected by a one millimeter optical collimator and transported *via* an optical fiber to the entrance slit of the monochromator. This device enables a spatial resolution in the plasma emissive cylinder of approximately 2 mm in diameter. The optical system was mounted on a computer controlled moving table, allowing axial and radial measurements. Emission intensities profiles, averaged on the line-of-sight, were measured at 90° to the axis of the reactor.

The Doppler broadened peak is a Gaussian and its FWHM is given by equation (1). Owing to the finite resolution of the spectrometer, the peak is a convolution of the line with the spectrometer response function. This latter has been approximated to a Gaussian function, and was determined using a low pressure mercury lamp (the natural broadening is known). We found $\Delta\lambda_{\text{opt.syst.}} = 6.5$ pm (0.0065 nm), which was confirmed later by a measurement using a He-Ne laser. Owing to the fine structure of the H_α line, a systematic decomposition of the spectrum must be done. According to Röpcke *et al.* [7], Vetterhöffer *et al.* [8] and Condon *et al.* [15], the spectrum has been decomposed in 7 Gaussian functions. For each of the components, the FWHM was obtained after substracting the optical system broadening.

The range of experimental conditions studied by OES is relatively large, in particular the pressure varies from 800 Pa to 14 000 Pa, and both Stark and pressure broadening have been taken into account. Then, the FWHM of each component is the result of the Gaussian Doppler broadening, the Lorentzian pressure broadening and the Lorentzian Stark broadening. According to [11, 16, 17], in hydrogen plasma, the pressure broadening is given by:

$$\Delta\lambda_p = \frac{n\sigma_{H_\alpha/H_2}\lambda_0^2 v_{H_\alpha/H_2}}{\pi} = 1.54\times 10^{-7}\lambda_0^2 n\sigma_{H_\alpha/H_2}\left(\frac{T_g}{\mu}\right)^{1/2} \tag{4a}$$

where n is the total density (in m^{-3}), v_{H_α/H_2} the relative mean velocity between H and H_2, σ_{H_α/H_2} the quenching cross section of H_α by H_2 molecules (in m^2), μ the reduced mass of H and H_2 (in g), and T_g the gas temperature. $\Delta\lambda_p$ is given in m. Owing to the dissociation of molecular hydrogen, the quenching term due to the collisions of H_α atoms with ground state

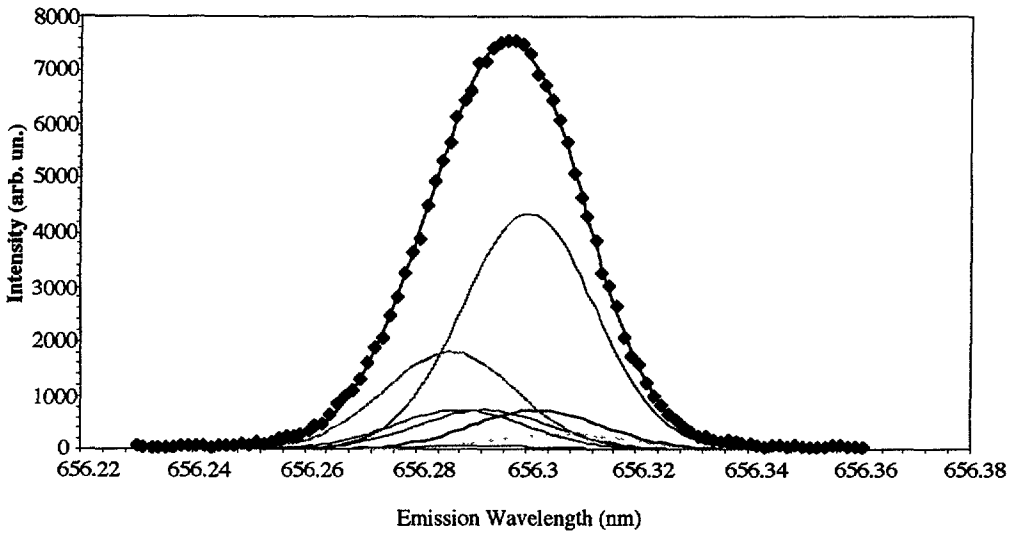

Fig. 3. — Experimental Doppler broadened spectrum of H_α transition obtained by OES. The decomposition in 7 features is shown.

H atoms must also be taken into account. The relation (4) becomes:

$$\Delta\lambda_p = 1.54 \times 10^{-7} \lambda_0^2 n(T_g)^{1/2} \left[(1 - x_H) \sigma_{H_\alpha/H_2} (\mu_{H/H_2})^{-1/2} + x_H \sigma_{H_\alpha/H} (\mu_{H/H})^{-1/2} \right] \quad (4b)$$

where μ_{H/H_2} represents the reduced mass of H and H_2 ($\mu_{H/H_2} = 2/3$), $\mu_{H/H}$ the reduced mass of H and H ($\mu_{H/H} = 1$), and x_H, the H-atom mole fraction determined experimentally [13]. The quenching cross section of H_α by H_2 molecules (σ_{H_α/H_2}) has been taken from Bittner *et al.* [18] and Prepperneau *et al.* [19]. The quenching cross section of H_α by H atoms ($\sigma_{H_\alpha/H}$) have been estimated at 18 Å^2 using the hard sphere model and taking the diameter cross section from literature [20, 21]. This value is however probably an upper value. $\Delta\lambda_p$ has been evaluated at less than 1 pm (0.001 nm) over the operating conditions used here.

The contribution of the Stark broadening has been estimated from the expression given by Wiese [15]:

$$\Delta\lambda_S = 5 \times 10^{-9} \alpha_{\frac{1}{2}} n_e^{2/3} \quad (5)$$

where n_e is the electron density (in cm^{-3}), $\alpha_{\frac{1}{2}}$ is depending on the principal quantum number (we took $\alpha_{\frac{1}{2}} = 0.018$ for the H_α line) [22] and $\Delta\lambda_S$ is given in Angström. Over the conditions used here, $\Delta\lambda_S$ has been estimated at up to 1.5 pm (0.0015 nm). A similar relationship for $\Delta\lambda_S$ is given by Griem [23, 24] ($\Delta\lambda_S = 2.507 \times 10^{-10} \alpha n_e^{2/3}$) with α, the Stark coefficient, equal to 0.00969. With this relationship, the Stark broadening is lowered by a factor 3.75 compared to that provided by the Wiese relationship.

An experimental broadened peak corresponding to the H_α emission is given in Figure 3, where the decomposition of the spectrum with the seven features is shown. After subtraction of the approximately Gaussian contribution of the optical system, the Lorentzian contributions were subtracted in order to determine the H_α temperature from Doppler broadening [25]. The Doppler broadening can also be determined by the subtraction of the Gaussian contribution of the optical system, and the Lorentzian contributions of pressure broadening and Stark

Table I. — *Calculated electron density as a function of the averaged power density.*

averaged injected power density (W cm^{-3})	pressure (Pa)	injected power (W)	n (10^{12} cm^{-3})	ΔStark (pm) (after Wiese)	ΔStark (pm) (after Griem)	Δpressure (pm)
6	1 400	400	1.31	1.08	0.287	0.136
9.2	2 500	600	1.18	1.00	0.268	0.200
15.3	5 200	1 000	1.24	1.04	0.277	0.368
22.9	8 500	1 500	1.46	1.16	0.309	0.501
33.6	10 000	2 200	2.06	1.46	0.389	0.493
36.6	14 000	2 400	2.07	1.46	0.390	0.655

broadening using the following approximated relationship [17]:

$$\Delta\lambda_{\text{mes}} = \frac{\Delta\lambda_{\text{L}}}{2} + \left(\frac{\Delta\lambda_{\text{L}}^2}{2} + \Delta\lambda_{\text{G}}^2\right)^{1/2} \tag{6}$$

where $\Delta\lambda_{\text{mes}}$ represents the measured width, $\Delta\lambda_{\text{L}}$ the Lorentzian contributions (Stark and pressure broadenings) and $\Delta\lambda_{\text{G}}$ the Gaussian contributions (Doppler and optical system broadenings). For each measurement of H_α-atom temperature, 9 spectra were recorded (each in 3 minutes), and an averaged value for the temperature was calculated. The error on the absolute measurement has been estimated at around 10% [26]. Note that only line-of-sight averaged H_α-atom temperature are available to date. The determination of real axial temperature would need a mathematical treatment of the line-of-sight signals (amplitude and width).

2.3. Determination of the Electron Density. — The electron density (n_e) was not accessible experimentally. It was estimated from the 1 dimensional H_2 plasma diffusive flow model developed at the laboratory. Table I gives the calculated electron density variation as a function of the power density calculated at 20 mm from the substrate. The error made on the electron density is mainly attributed to the power effectively absorbed by the plasma, and to the assumption that the electron energy distribution function is Maxwellian. Recent calculations [27] carried out without assuming a Maxwell distribution for the electron energy, indicate that n_e is overestimated by 20 to 35% when assuming a Maxwell distribution. The error made on the absorbed power has been estimated at 10%.

At 9 W cm^{-3} (600 W and 2 500 Pa), the variation of the electron density as a function of the methane percentage was estimated from (i) the electron density calculated in absence of methane, (ii) the variation of the argon emission intensity as a function of the percentage of methane added in the feed gas (Fig. 4). As a matter of fact, as the percentage of methane was increased up to 5%, no variation of the ratios of emission intensities of different lines of H atoms (H_α, H_β, H_δ and H_γ) was observed, and we concluded that the electron temperature can be considered as a constant, at least in first approximation. As a consequence, the variation of the argon emission intensity depends only on the electron density.

3. Results and Discussion

3.1. Variations as a Function of the Methane Percentage. — The H-atom temperatures (T_H) were measured as a function of the CH_4 percentage introduced in the feed gas at a distance of 20 to 25 mm from the diamond substrate, in a region where the axial gradients are negligible [6, 10, 12, 13]. This region is defined as the bulk of the plasma (plasma

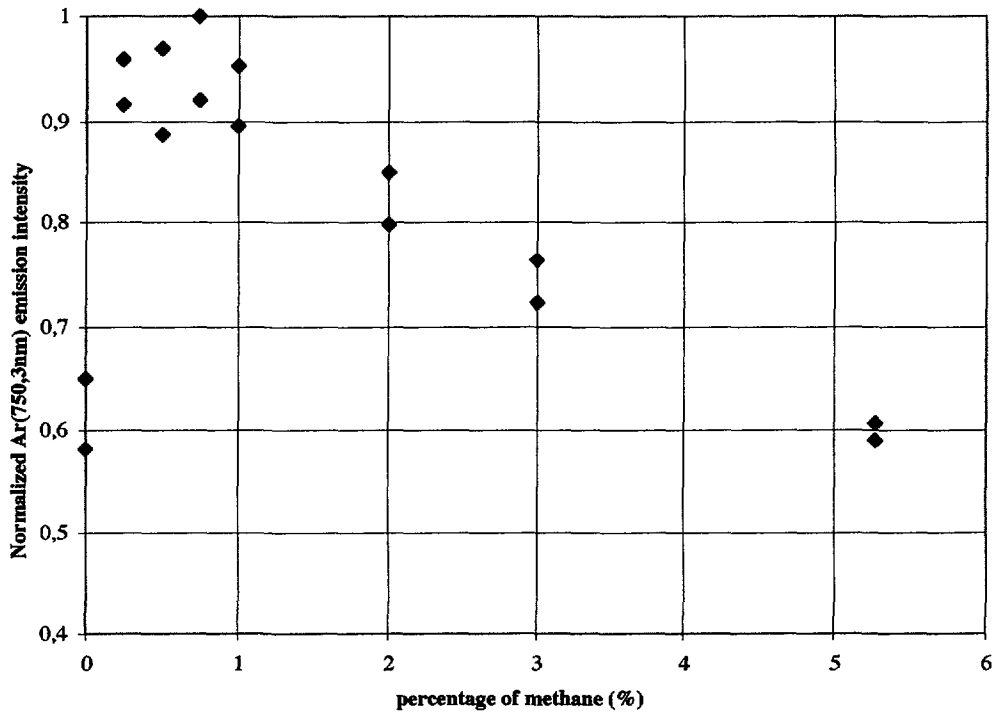

Fig. 4. — Variation of the averaged line-of-sight emission intensity of argon (λ = 750.3 nm) as a function of a low percentage of CH_4 in a hydrogen plasma containing 1% argon. Plasma conditions: 600 W, 2500 Pa, 9 W cm^{-3}, 300 sccm, T_s = 900 °C. Measurements are made at 20 mm from the substrate (in the bulk of the plasma).

volume) in contrast to the plasma/surface interface where strong gradients are characteristics of the thermal boundary layers. The temperatures T_H are compared to the $H_2(X)$ rotational temperatures ($T_R H_2(X)$) measured previously by CARS at the same averaged power density (9 W cm^{-3}) and at the same location [12, 13]. Whatever the percentage of methane, T_H is equal to $T_R H_2(X)$, that is to the gas kinetic temperature. As the percentage increases from 0 to 5%, it remains constant at around 2 150 K (Fig. 5). Note that the H-atom temperatures measured by TALIF are more scattered than $T_R H_2(X)$.

The "line-of-sight averaged H_α-atom temperature", can be deduced from the experimental H_α peak FWHM (measured by OES) assuming first that the broadening is only Doppler dominated. In the bulk of the plasma (at 20 mm far from the substrate holder), it (T_{H_α} without corrections) is rather constant as a function of the percentage of methane introduced in the feed gas (Fig. 6). It is around 150 K to 200 K higher than the gas temperature. Using relations (4b) and (5), we can estimate the contributions of the pressure and Stark broadenings to the H_α-FWHM. The corrected temperatures (T_{H_α} pressure and Stark effects corrected) are reported in Figure 6. T_{H_α} is equal to the gas temperature and remains at the value of 2 200 K as the percentage of methane introduced is varying up to 5% (within the experimental error). Gas temperature can then be deduced from measurement of the H_α line broadening, when taking into account for the pressure and Stark effect broadenings, under these experimental conditions. Note that, at this pressure (2 500 Pa), the Stark contribution is almost 10 times the pressure contribution.

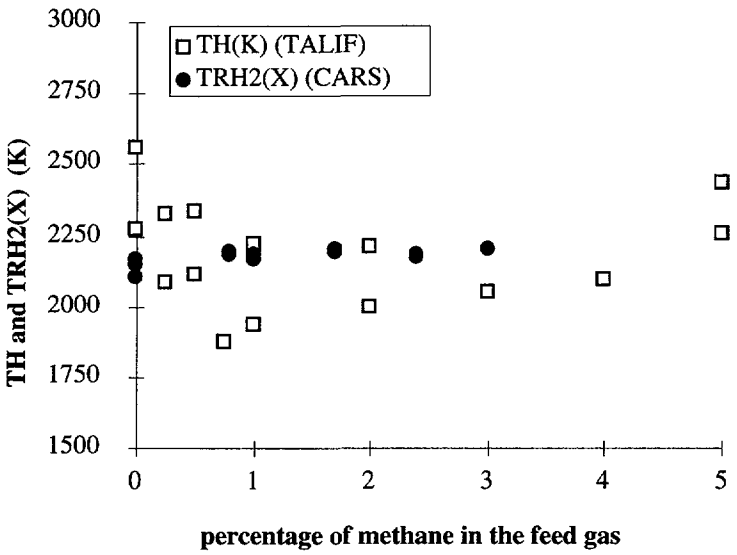

Fig. 5. — Variations of the $H_2(X)$ rotational temperature (CARS) [2,3] and H-atom temperature T_H (TALIF) as a function of a low percentage of methane in the feed gas, measured at 20 to 25 mm from the substrate, in the plasma volume (bulk of the plasma). Plasma conditions: 600 W, 2500 Pa, 9 W cm^{-3}, 300 sccm, $T_s = 900$ °C.

3.2. Variations as a Function of the Microwave Power Density. — The variations of T_H, measured at 25 mm from the substrate (bulk of the plasma), as a function of the averaged microwave power density are presented in Figure 7. T_H increases from 1550 ± 180 K to 2600 ± 300 K as the power density increases from 6 to 15 W cm^{-3}. The variation of T_H is compared to that of the gas kinetic temperature, calculated using the 1D diffusive non equilibrium H_2 plasma model [10,11], which is reported in Figure 7. There is a very good agreement between the measured and the calculated gas temperatures, for the range of power densities where T_H was measured (< 15 W cm^{-3}). At 30 W cm^{-3}, the calculated gas temperature in the bulk of the plasma reaches 3 100 K.

The "line-of-sight averaged H_α-atom temperature", deduced assuming first that the broadening is only Doppler dominated (T_{H_α} without corrections) varies from 1680 ± 170 K to $3\,900 \pm 400$ K as the power density varies from 4.5 to almost 37 W cm^{-3} (Fig. 8) (measured in the bulk of the plasma at 20 mm far from the substrate holder). The higher the power density, the higher the difference between " T_{H_α} without corrections" and the calculated gas temperature. Taking into account for the pressure and Stark effects, T_{H_α} varies from 1610 K $\pm$ 150 K to around 3 600 K $\pm$ 350 K as the power density increases from 4.5 to 37 W cm^{-3} (Fig. 8). T_{H_α} is almost identical to the gas temperature for power densities up to around 25 W cm^{-3}, while it seems to increase slightly faster than T_g for higher values of the power density. At 37 W cm^{-3}, the lower limit value of measured T_{H_α} (taking account for the error bar) is 100 K higher than the calculated T_g. However, owing to the 10% error made on the power density, when considering the error bars, we can conclude that T_g is still within the T_{H_α} error bar.

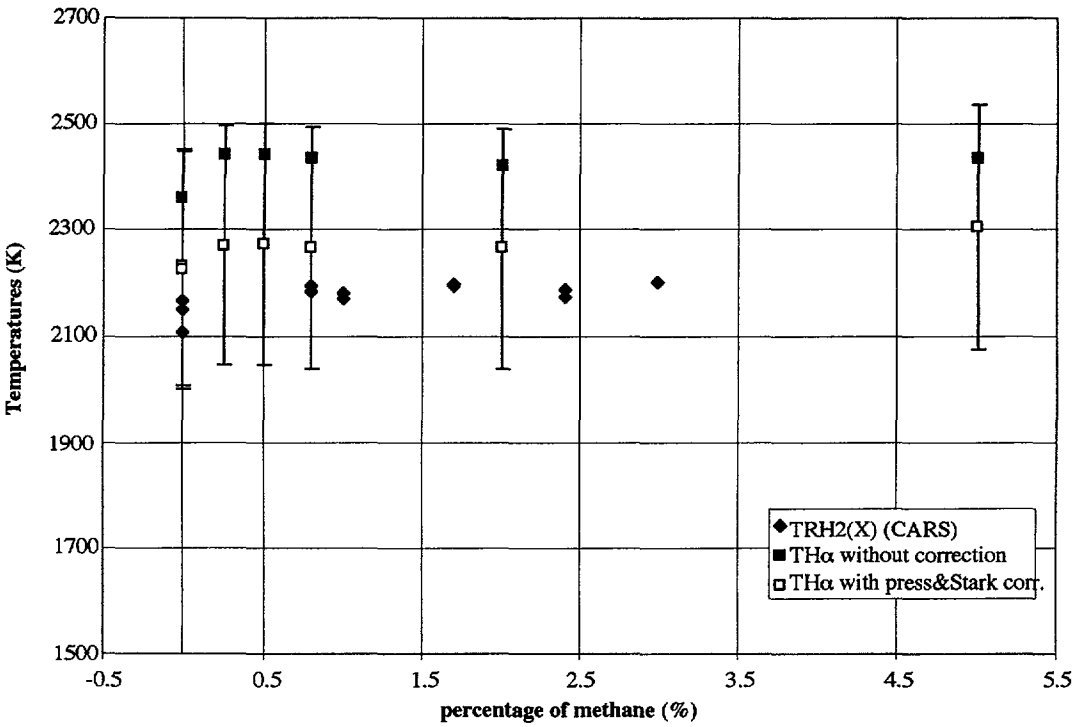

Fig. 6. — Variations of $H_2(X)$ rotational temperature measured by CARS and line-of-sight T_{H_α} measured from line broadening (OES) as a function of the percentage of methane introduced in the feed gas. Measurements are carried out at distances of 20 to 25 mm from the substrate, in the plasma volume. T_{H_α} (without corr.) represents the temperature deduced assuming that the line broadening is only Doppler dominated. T_{H_α} (with Press & Stark corr.) represents the temperature deduced when, beyond Doppler broadening, pressure and Stark broadenings are considered. Plasma conditions: 600 W, 2500 Pa, 9 W cm^{-3}, 300 sccm, $T_s = 900$ °C.

3.3. Discussion

Stark effect. — According to the calculations carried out assuming a Maxwell distribution for the electrons energy, the Stark broadening estimated from the Wiese relationship varies from 1 pm up to 1.46 pm as the power density increases from 6 to 37 W cm^{-3} (Tab. I). The effect of this broadening is to lower the " T_{H_α} without corrections" by 100 K to almost 200 K as the power density increases in the range of conditions studied here. Calculations assuming a non-Maxwellian distribution for the electron energy indicates that the electron density is overestimated by 20 to 35% when considering a Maxwellian distribution. 100 K to 200 K represent then the upper limits of the Stark broadening effect on T_{H_α} measurements.

The Griem relationship leads to lower Stark broadening effects on T_{H_α} (50 K to 60 K). These values can be taken as lower limits of the Stark broadening effect on T_{H_α} measurements.

Pressure Effect. — Under microwave plasma diamond deposition conditions, pressure broadening was seen to be non negligible for the determination of the H_α-atom temperature, although less than the Stark broadening (using the Wiese's relationship). As the power density increased

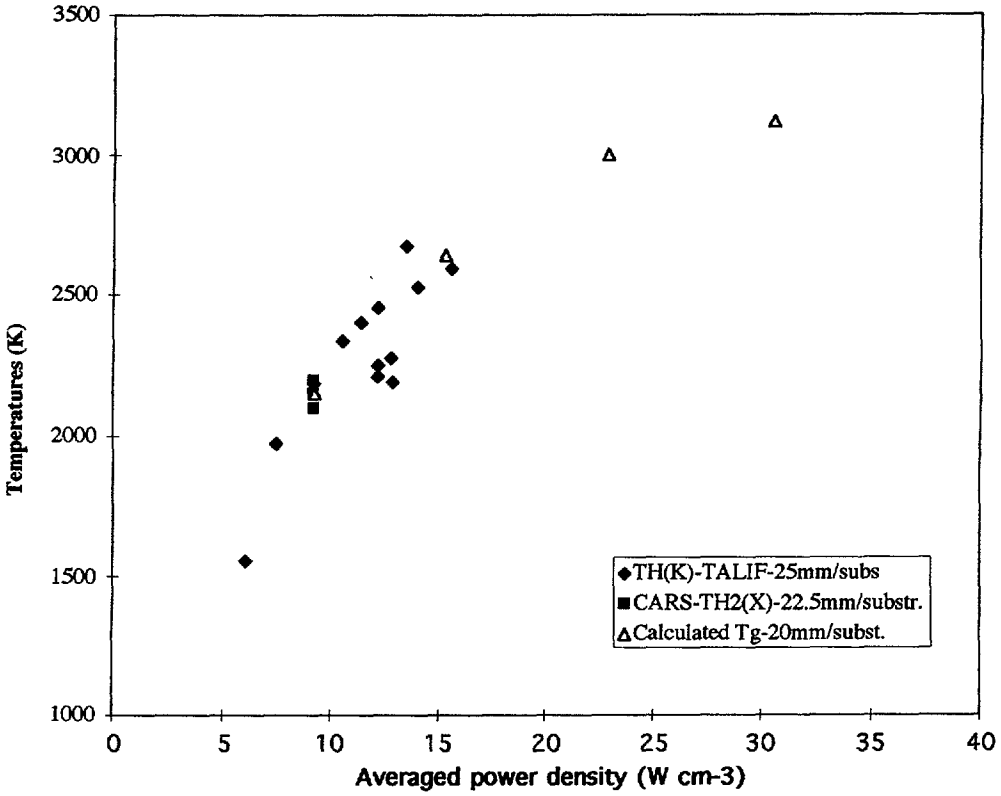

Fig. 7. — Variations of H-atom temperature T_H (measured by TALIF), $H_2(X)$ rotational temperature (measured by CARS), and calculated gas kinetic temperature (with a 1D diffusive H_2 plasma flow model), in a pure hydrogen plasma, as a function of the averaged injected power density. Measurements are all performed in the plasma volume (bulk) at 20 to 25 mm from the substrate.

from 9 to 34 W cm^{-3} (the pressure increased from 2 500 Pa to 12 000 Pa), the pressure broadening was seen to vary from 0.14 to 0.65 pm. The consequence of the pressure broadening is a lowering of the " T_{H_α} without corrections" by 20 K to 60 K, according to the experimental conditions.

Comparison Between Experimental Values and Calculated Temperatures. — Over the whole range of power densities studied here (4.5 W cm^{-3} to 37 W cm^{-3}, with pressure ranging from 1 400 Pa to 14 000 Pa), owing to the large uncertainties, H_α-atom temperature can be considered as in equilibrium with both ground state H-atom temperature and gas temperature. As the pressure and the power increase (the power density increases), all the temperatures, *i.e.* the gas temperature, T_{H_α}, and also the electronic excited G state of hydrogen molecules rotational temperature (as shown in Ref. [6]), tend towards a plateau. The presence of the plateau is attributed to the strong thermal dissociation processes which occur at temperatures ranging from 3 000 K to 3 500 K, and consume a large part of the microwave power.

The fact that the excited H-atoms temperature is equal to ground state H-atom temperature, over this range of conditions is the consequence of the processes occurring under these experimental conditions which strongly differ from the one occurring in low pressure plasmas. Owing

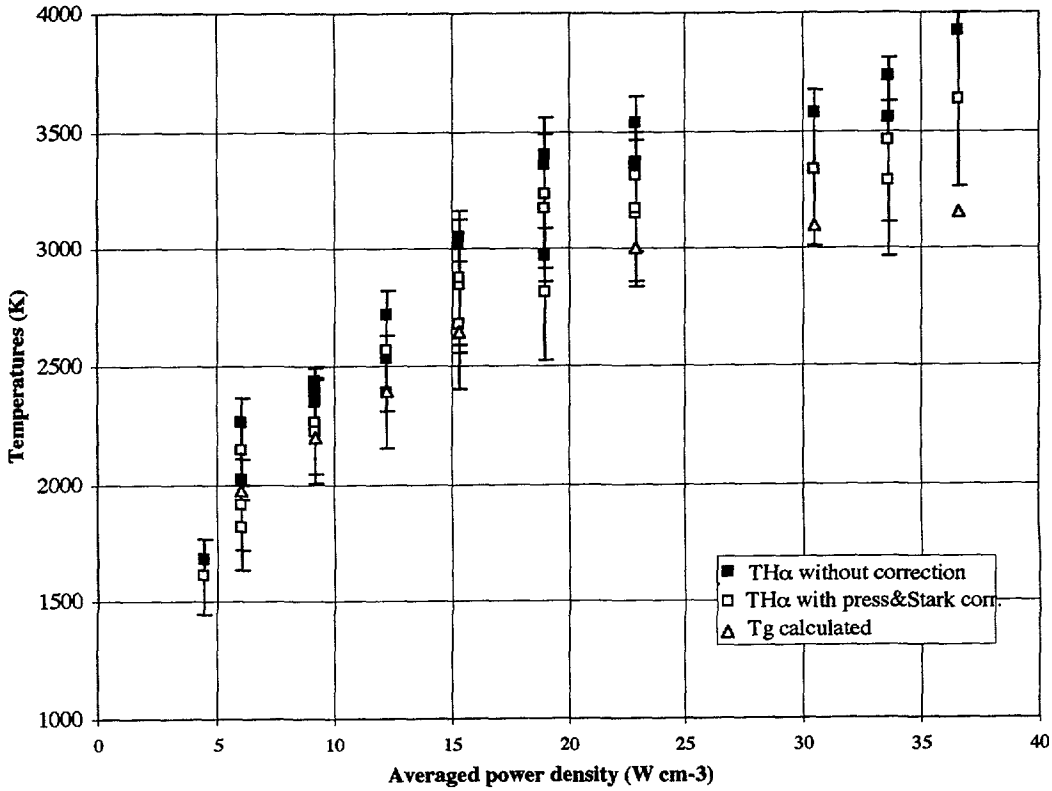

Fig. 8. — Variations of calculated gas kinetic temperature (with a 1D diffusive H_2 plasma flow model), and line-of-sight T_{H_α} measured from line broadening by OES as a function of the averaged injected power density. The measurements are carried out in the plasma volume (bulk). T_{H_α} (without corr.) represents the temperature deduced assuming that the line broadening is only Doppler dominated. T_{H_α} (with Press & Stark corr.) represents the temperature deduced when, beyond Doppler broadening, pressure and Stark broadenings are considered.

to the rather low electron temperature (1 to 2 eV) and to the high gas temperatures characterizing diamond deposition conditions, the main part of H atoms formed in these reactors is produced by thermal dissociation of molecular hydrogen while, in microwave plasma operating at around 100 Pa, it occurs through electron collisions with H_2 molecules [1,4]. In diamond reactor, the consequence is that the $n = 3$ excited H atoms are mainly populated directly from the ground state H atoms by collisions with electrons. In addition, the high collisional frequency lead to high energy transfer rates between molecules and atoms, and to a thermal equilibrium between the atoms and the molecules in their ground electronic states. Also the production of some very hot H_α atoms by strongly energetic repulsive dissociative excitation processes (threshold at around 27 eV) [28,29] is unrealistic in these plasmas. In addition, the higher the pressure, the less the contributions of both direct electron impact dissociation and dissociative excitation mechanism, owing to the decrease in the electron temperature (calculations [10,11]).

Although, over the whole range of experimental conditions studied here, T_{H_α} can be considered as equal to T_g, for power densities higher than 25 W cm^{-3}, T_{H_α} was seen to increase slightly faster than the calculated T_g. Uncertainties in the calculated gas temperatures might

also be invoked. They can be attributed to the assumptions made for building the models. Plasma models are being improved today in order to couple the H_2 plasma diffusive flow to (i) the Boltzmann equation for the electrons, (ii) the Maxwell equations for knowing the exact distribution of the electromagnetic field, (iii) the Navier-Stokes equations for taking into account for the convection which might be important at high power density (natural convection). Further temperatures measurements are also still in progress in the laboratory.

4. Conclusion

Under typical conditions used for diamond deposition, we have measured H-atom temperature in ground state and in the $n = 3$ excited state (H_α) from the Doppler broadening, using TALIF and OES respectively. They have been compared to the ground state rotational temperature of molecular hydrogen measured by CARS under the same conditions, and to the gas kinetic temperature calculated with a 1D diffusive model developed for a non-equilibrium H_2 plasma.

Line-of-sight averaged H_α-atom temperatures (T_{H_α}), measured by OES, showed that, under diamond deposition conditions, Doppler, pressure and Stark broadenings are contributing to the FWHM. Although the contribution of the Stark broadening on T_{H_α} is higher than the pressure contribution, its importance differs from an author to another.

Owing to the uncertainties, the H_α-atom temperature was seen to be rather in thermal equilibrium with the ground state H-atom temperature and with the ground electronic state molecules rotational temperature (gas temperature). The temperatures were seen to be strongly sensitive to the power density and to increase from 1 550 K to almost 3 200 K as the power density is increased from 4.5 to 37 W cm^{-3} A plateau was observed after 25 W cm^{-3}, which has been attributed to the thermal dissociation processes which are very efficient at temperature of 3 100 K. At a power density of 9 W cm^{-3}, the temperatures remain constant at 2 150 – 2 200 K, as a percentage of methane up to 5% is introduced in the feed gas.

Measurements of T_{H_α} constitutes probably today one of the best way for approaching the gas kinetic temperature by OES in diamond deposition reactors. Nevertheless, further measurements as well as calculations using more sophisticated models of H_α-atom temperature are still necessary, in particular at high power densities.

Acknowledgments

This work was financially supported partially by DRET. Michel Lefebvre from ONERA is thanked for the CARS measurements, Jean-Christophe Cubertafon for its contribution to TALIF measurements and Antoine Rousseau from CNRS-ORSAY for helpful discussions.

References

[1] de Amorim Filho J., *J. Appl. Phys.* **76** (1994) 1487-1493.
[2] de Amorim Filho J., PhD thesis, Université d'Orsay (Paris XI, 1994).
[3] Dunlop J.R., Tserepi A.D., Prepperneau B.L., Cerny T.M. and Miller T.A., *Plasma Chem. Plasma Process.* **12** (1992) 89-101; Prepperneau B.L., Optical diagnostics in a diamond deposition reactor, École Diagnostics plasma (Les Houches, Janvier 1995).
[4] Tomasini L., Rousseau A., Gousset G. and Leprince P., *J. Phys. D: Appl. Phys.* **29** (1996) 1-8.
[5] Chenevier M., Cubertafon J.C., Campargue A. and Booth J.P., *Diam. Rel. Mater.* **3** (1994) 587-592.

[6] Gicquel A., Chenevier M., Hassouni K., Breton Y. and Cubertafon J.C., *Diam. Rel. Mater.* **5** (1996) 366-372.
[7] Röpcke J. and Ohl A., *Contributed Plasma Physics* **34** (1994) 575-586; Ito K., Oda N., Hatano Y. and Tsuboi T., *Chem. Phys.* **17** (1976) 35-43.
[8] Vetterhöffer J., Campargue A., Stoeckel F. and Chenevier M., *Diam. Rel. Mater.* **2** (1993) 481-485.
[9] Lang T., Stiegler J., Von Kaenel Y. and Blank E., *Diam. Rel. Mater.* (1996) to be published.
[10] Hassouni K., Farhat S., Scott C. and Gicquel A., *J. Phys. III France* **6** (1996) 1229.
[11] Hassouni K., Scott C. and Farhat S., Chapter "Modelling and diagnostics in plasmas" - Section 7.1- Handbook for Industrial Diamonds and Diamond Films, M. Prelas, G. Popovicci and K. Bigelow Eds., to be published (1996).
[12] Gicquel A., Hassouni K., Farhat S., Breton Y., Scott C.D., Lefebvre M. and Pealat M., *Diam. Rel. Mater.* **3** (1994) 581-586.
[13] Gicquel A., Chenevier M. and Lefebvre M., Chapter "Modelling and diagnostics in plasmas"- Section 7.2 - Handbook for Industrial Diamonds and Diamond Films, M. Prelas, G. Popovicci and K. Bigelow Eds., to be published (1996).
[14] Tan W. and Grotjohn T., *Jac. Sci. Technol. A* **12** (1994) 1216-1220.
[15] Condon E. U. and Shortley G. H., Theory of atomic spectra (Cambridge Unversity Press, Cambs, 1959).
[16] Demtroder W., Laser Spectroscopy. Basic concepts and Instrumentation, Volume 5 of Series in Chemical Physics (Springer-Verlag edition, 1981).
[17] "Les Applications Analytiques des Plasmas HF", C. Tracy and J.M. Mermet, Eds., Technique et Documentation (Lavoisier, 1984).
[18] Bittner J., Kohse-Höinghaus K. and Meier U., *Th. Just. Chem. Phys. Letters* **143** (1988).
[19] Prepperneau B. L., Pearce K., Tserepi A., Wurzberg E. and Miller T. A., *Chemical Physics* **196** (1995) 371-381.
[20] Matsui Y., Yuuki A., Morita N. and Tachibana K., *Jpn J. Appl. Phys.* **26** (1987) 1575.
[21] Kushner M.J., *J. Appl. Phys.* **63** (1988) 2532.
[22] Wiese W.L., Plasma Diagnostics Techniques-Pure and Applied Physics (21), R.H. Huddlestone and S.L. Leonard, Eds. (Academic Press, 1965).
[23] Blau P., Smilanski I. and Rosenwaks S., *J. Appl. Phys.* **72** (1992) 849-854.
[24] Griem H.R., Spectral line broadening by plasma (Academic Press, New York, 1974).
[25] Posener D.W., The shape of spectral lines: tables of the Voigt profiles, *Australian J. Phys.* **12** (1959) 184.
[26] Griem H.R., Plasma Spectroscopy (Mac Graw Hill Book Company, 1964).
[27] Scott C., Farhat S., Hassouni K. and Gicquel A., Internat. Symposium on Diamond Films 3 (St Petersbourg, June 1996).
[28] Sultan G., Baravian G., Gantois M., Henrion G., Michel H. and Ricard A., *Chem. Phys.* **123** (1988) 423-429.
[29] Robin F., PhD Thesis, Université Paris XI (Orsay, 1990).